Article:
Martelli, S., Valente, G., Viceconti, M. et al. (2015) Sensitivity of a subject-specific musculoskeletal model to the uncertainties on the joint axes location. Computer Methods in Biomechanics and Biomedical Engineering, 18 (14). pp. 1555-1563. ISSN: 1025-5842

https://doi.org/10.1080/10255842.2014.930134

Sensitivity of a subject-specific musculoskeletal model to the uncertainties on the joint axes location

Saulo Martelli[a *], Giordano Valente[b,c] , Marco Viceconti[d] and Fulvia Taddei[b]

a) School of Computer Science, Engineering and Mathematics, Medical Device Research Institute, Flinders University, Bedford Park,South Australia, Australia;

b) Laboratorio di Tecnologia Medica, Istituto Ortopedico Rizzoli, Bologna, Italy;

c) Department of Industrial Engineering, University of Bologna, Bologna, Italy; d Department of Mechanical Engineering and Insigneo Institute for in Silico Medicine, University of Sheffield, Sheffield, UK

Corresponding author:
Dr Saulo Martelli
Medical Device Research Institute
School of Computer Science, Engineering and Mathematics
Flinders University
Email: saulo.martelli@flinders.edu.au
Postal details:
Sturt Road, Bedford Park, South Australia, 5042
GPO Box 2100, Adelaide SA 5001

Abstract

Subject-specific musculoskeletal models have become key tools in the clinical decision-making process. However, the sensitivity of the calculated solution to the unavoidable errors committed while deriving the model parameters from the available information is not fully understood. The aim of this study was to calculate the sensitivity of all the kinematics and kinetics variables to the inter-examiner uncertainty in the identification of the lower limb joint models. The study was based on the computer tomography of the entire lower-limb from a single donor and the motion capture from a body-matched volunteer. The hip, the knee and the ankle joint models were defined following the International Society of Biomechanics recommendations. Using a software interface, five expert anatomists identified on the donor's images the necessary bony locations five times with a three-day time interval. A detailed subject-specific musculoskeletal model was taken from an earlier study, and re-formulated to define the joint axes by inputting the necessary bony locations. Gait simulations were run using OpenSim within a Monte Carlo stochastic scheme, where the locations of the bony landmarks were varied randomly according to the estimated distributions. Trends for the joint angles, moments, and the muscle and joint forces did not substantially change after parameter perturbations. The highest variations were as follows: (a) 118 calculated for the hip rotation angle, (b) 1% BW £ H calculated for the knee moment and (c) 0.33 BW calculated for the ankle plantarflexor muscles and the ankle joint forces. In conclusion, the identification of the joint axes from clinical images is a robust procedure for human movement modelling and simulation.

Keywords: musculoskeletal model; hip load variation; muscle force sensitivity; joint axes uncertainty; gait simulations; human motion

Introduction

In the last decade, musculoskeletal models have evolved from exclusively research tools to clinical methods used in the decision-making process (Jonkers et al. 2008). In this new context, subject-specific models, typically generated from heterogeneous data such as clinical images, published atlases and direct anthropometrical measurements, are key factors in the calculation of reliable mechanical variables (Lenaerts et al. 2008; Lenaerts et al. 2009; Scheys et al. 2008; Valente et al. 2012). For example, subject-specific models were found to be key factors for an accurate calculation of muscle lever arms (Lenaerts et al. 2008; Valente et al. 2012), skeletal forces (Lenaerts et al. 2008), bone stresses (Jonkers et al. 2008), and for properly addressing the related clinical implications (Steele et al. 2012; Taddei et al. 2012). However, the error committed in extracting the model parameters from the available clinical information affects the calculated variables in a way that needs to be investigated.

The model identification process involves several and fairly complex operations (Scheys et al. 2009; Taddei et al. 2012). For instance, the inertial parameters can be derived from simple anatomical measurements using regression equation with not less than a 21.3% error on one or more parameters (Durkin and Dowling, 2006). The muscle attachment locations can be automatically estimated from Magnetic Resonance Images (MRI) with an average error of 6.1 mm (Scheys et al. 2009). The hip joint center location can be determined using a functional method from simple recordings of the hip motion or, as a possible alternative, using regression equations from simple measurements that can be easily taken on the patient skin. The functional method was able to estimate the hip joint center with an average error of 13 mm, whilst regression equations showed a higher average error up to 30 mm (Leardini et al. 1999). The skeletal geometry is often extracted from clinical images with an error in the order of at least two pixels (Testi et al. 2001). The joint axes of the knee and the ankle can be defined using the location of prominent bony landmarks lying on each respective joint axis (Grood & Suntay 1983; Wu et al. 2002). To this purpose, a computer- based procedure, the so-called Virtual Palpation procedure, has been recently proposed to locate all the necessary bony landmarks on the available clinical images with an uncertainty up to 3 mm (Taddei et al. 2007). Whatever the adopted identification process is, the errors committed clearly alter the calculated variables in a way that is not known a-priori.

Several authors investigated the sensitivity of calculated skeletal forces to changes of the model parameters. Changes of the muscle physiological cross section area (PCSA) within the physiological range led to 11% variation of the hip force (Brand et al. 1986) and up to more than 100% variation of the calculated muscle forces (Brand et al. 1986; Herzog 1992). Xiao & Higginson (2010) perturbed selected muscle parameters (i.e., the number of muscle lines of action, the maximum isometric force, the optimal fiber length and the tendon slack length) by a ±10% factor, showing variations in the calculated muscle forces up to 12.8 times the magnitude of the imposed parameter perturbations. Scaling a general pelvis model on personalized anthropometric information can induce an up to 3 cm misallocation of the hip and a consequent shift of the calculated hip force in the order of 0.5 times body weight (BW) (Lenaerts et al. 2009). The position in the body segments of the joint axes affects the calculation of muscle and joint forces by influencing the calculation of the joint torques and the muscle's lever arm. However, no studies reported on the sensitivity of the calculated muscle and joint forces to the uncertainty associated to the identification of the lower-limb joint axes with clinical images available.

The aim of this study is to estimate the sensitivity of the muscle and joint forces associated with inter-examiner uncertainty in locating the relevant skeletal landmarks (Grood & Suntay 1983; Wu et al. 2002) defining the lower-limb joint axes. To this aim, the uncertainty on the landmark positions was assessed, and its effect on the skeletal forces calculated using optimization theory was estimated by means of a subject-specific musculoskeletal model of the lower limbs, performing a Monte Carlo stochastic analysis.

Materials and methods

The study was based on a whole-body CT dataset from a single donor and the motion data from a body-matched volunteer. Five expert anatomists identified the necessary bony landmarks using the Virtual Palpation procedure (Taddei et al. 2007), providing the necessary measurements for the estimation of the probability density distribution of the landmark locations. A musculoskeletal model was taken from an earlier study (Martelli et al. 2011), and reformulated in a parametrical way to define the articular joints from the necessary landmark locations. A Monte Carlo stochastic scheme was used to generate an adequate set of joint models from the estimated distributions. A standard software pipeline (OpenSim (Delp et al. 2007), www.simtk.org) was used to calculate the body kinematics, the joint moments and the muscle and joint forces for a selected stride. Results were post-processed to expose the variations of calculated parameters.

The CT dataset and the motion data

The CT dataset was taken from an 81-year-old donor (female, 167 cm height and 63 kg weight) during an earlier study (Viceconti et al. 2008). The dataset was recorded with a clinical scanning machine (manufacturer: Siemens Medical Solutions USA, Inc., model: Sensation 64) using common physical parameters (tube voltage: 120 kVp, tube current: 270 mA). The dataset included the entire lower limbs, from the entire pelvis down to the entire feet. The pixel size was 0.9765 mm while the spacing was 1 mm. The body motion was recorded from a body-matched volunteer (female, 25 years old, 165 cm height and 57 kg weight) following the gait analysis protocol proposed by Leardini et al. (2007), which provided 3D motion (Vicon Motion Capture, Oxford UK) of the lower limb segments (sampling rate 100Hz) and the ground reaction forces at both feet (sampling rate 2000Hz). Bilateral motion and ground reaction forces were recorded for consecutive right and left steps during walking at normal speed. Both the CT dataset and the motion data are freely available for download at www.physiomespace.com (Testi et al., 2010).

Estimation of the joint centres and axes

The joint centres and axes were defined according to the International Society of Biomechanics (ISB) (Wu et al. 2002) using the location of relevant bony landmarks. The bony locations necessary to identify the hip, the knee, and the ankle model were the hip center (HC), the lateral epicondyle (LE), the medial epicondyle (ME), the lateral malleolus (LM), and the medial malleolus (MM). The HC location was estimated by visually identifying the sphere that best fitted the femoral head surface, through a multimodal visualization approach allowing a combined 3D visualization of the CT volume and the skeletal surface (Taddei et al. 2007). The femoral epicondyles and the tibio-fibular malleoli were located by picking the selected location on the skeletal surface extracted from the CT images. Five expert anatomists located the full set of bony locations on both legs using a dedicated software environment (LHPBuilder, SCS, Italy). Each anatomist repeated all the measurements three times with a time interval of three days.

The parametric musculoskeletal model

The base musculoskeletal model is extensively described in an earlier work (Martelli et al. 2011). The biomechanical model was defined as a 7-segment, 10 degree-of-freedom (DOFs) articulated system, actuated by 82 muscle-tendon units. Three ideal joints articulated each leg: a ball-and-socket (3 DOFs) at the hip and a hinge (1 DOF) at both the knee and the ankle. A well-established muscular model of the lower extremity (Delp et al. 1990) was manually registered on the subject-specific anatomy by an expert anatomist. In the earlier study (Martelli et al. 2011), the model was validated showing a good agreement between the calculated muscle and hip forces with, respectively, the available EMG recording and published measurements of hip force (Figure 1). In the present study, the model was re-written in a parametric form using an in-house routine (Matlab © , The Mathworks Inc., USA) to allow the definition of the joint axes from the necessary landmark locations. Specifically, the knee axis was defined from ME and LE locations, assuming the knee axis passing through the two bony locations and the knee centre as the midpoint between the two (Grood & Suntay 1983). Similarly, the ankle axis was defined from MM and LM locations, assuming the ankle axis passing through the two bony locations and the ankle centre as the midpoint between the two (Wu et al. 2002).

[Figure 1 near here]

The Probabilistic Design

The AP (antero-posterior) and the CC (cranio-caudal) coordinates of the femoral epicondyles and the tibio-fibular malleoli were defined as normally distributed variables. The mean position and the standard deviation of the femoral epicondyles and the tibio-fibular malleoli were assigned the mean position and the variance from the available measurements. The hip joint centre, the medio-lateral position of the femoral epicondyles, and the medio-lateral position of the tibio- fibular malleoli were assigned deterministic values, equal to the mean identified locations. A Latin Hypercube Sampling technique (LHS), which is a more efficient form of a Monte Carlo simulation method, was applied using Matlab © (The Mathworks Inc., USA). The algorithm was used to randomly generate an appropriate set of bony locations, known as the “sampling points” hereinafter, which were distributed in space according to the probability distribution estimated from the five anatomists’ measurements. The number of the necessary sampling points was determined by checking convergence of all the input and output variables, including marker positions, joint angles, joint moments, muscle and joint forces. Convergence was assumed when the inclusion of an additional sampling point induced changes of the standard deviation $< 2\%$ and of the mean value $< 0.2\%$.

The calculation of the skeletal kinematics, kinetics, and the muscle and joint forces

The musculoskeletal model was input with each sampling point, and the gait cycle was simulated using a standard pipeline, including inverse kinematics, inverse dynamics, static optimization and joint reaction analysis (Delp et al. 2007). The static optimization analysis was conducted to decompose the joint moments into muscle forces by minimizing the sum of the squared muscle activation. The time histories of all the kinematics, the kinetics, and the muscle and joint forces were calculated and normalized in terms of percentage of gait cycle. Calculated forces were normalized in terms of body weight (BW) whilst calculated moments were normalized in terms of percentage of body weight times subject height (%BW*H). The muscle forces were grouped according to their main function (Table 1) and compared by swapping swing and stance phase in the left leg. The variation range of the calculated distributions was presented for the joint kinematics, moments, and calculated forces. All the analyses were performed using Matlab © (The Mathworks Inc., USA).

[Table 1 near here]

Results

Estimation of the joint centres and axes

The standard deviation of the hip centre coordinates was lower than 0.4 mm. The standard deviation for the LM, MM, LE and ME positions along the antero-posterior and cranio-caudal coordinates was lower than 2.3 mm while along the medio-lateral coordinate was lower than 0.5 mm. The resulting variation of the knee and ankle axes orientation was less than 2° and 0.4°, respectively (Table 2).

[Table 2 near here]

Convergence analysis

For all the investigated input and output variables, 400 runs were sufficient to reach an asymptotic plateau ensuring convergence of all the input and output variables. Joint forces required the higher number of sampling points to reach convergence; Figure 2 shows the convergence pattern for the knee contact force, the variable that reached convergence after all the 400 runs.

[Figure 2 near here]

Uncertainties on joint kinematics, joint moments, and joint and muscle forces

The variation of all the kinematics and kinetics variables showed similar patterns for both legs. Throughout stride, all the joint angles never exceeded 5.4 degrees variation with the only exception for the hip rotation angle, which reached 11 degrees variation during mid-swing (Figure 3). The variation of the hip moments never exceeded 0.5 %BWxH for the adduction, the flexion and the rotation axis, with peak variations predicted during the stance-to-swing and swing-to-stance transition phases. The variation of the knee moment was up to 1 %BWxH, calculated during late stance, whilst the variation of the ankle moment was up to 0.72 %BWxH calculated, again, during late stance (Figure 4).

[Figure 3 and 4 near here]

Patterns for the principal muscle groups and the joint forces were consistent for legs, either in terms of magnitude and timing (Figure 5), showing the tendency for moderately higher variations during early and late stance, synchronously with peak variations of the joint moments (Figure 6). The highest variation of muscle forces was 0.33 BW, calculated during early stance for the ankle plantarflexors. The peaks of the force variations at the joints were 0.26 BW at the hip, 0.16 BW at the knee, and 0.33 BW at the ankle.

[Figure 5 and 6 near here]

Variation of the joint forces never exceeded the 9% of the peak force calculated for the same joint while variation of the muscle group forces reached for the hip flexors the 114% of the hip flexors's peak force.

Discussion

Modelling the patient musculoskeletal system has become important in the clinical decision-making process (Jonkers et al. 2008), stimulating the emergence of methodologies to identify the model parameters from the available clinical information. However, the effect on the calculated variables of the unavoidable errors committed during the model identification process is not fully elucidated. The aim of the study was to estimate the variability of the calculated muscle and joint forces due to the inter-examiner uncertainty in locating the necessary bony locations.

Variations in the bony landmark locations induced generally small variations of all the investigated variables, not substantially altering the calculated patterns. Indeed, the calculated variations of the joint angles were in average 2.3 degrees, and never exceeded the 11 degrees calculated for the hip rotation angle. Variations of the joint moments never exceeded the 11 % of the peak moment. Grouping muscle and joint forces together, variations never exceeded the 0.33 BW, a value that represents the 8-10% of the peak joint forces, which ranged from 3.44 BW at the hip to 4.04 BW at the ankle. This uncertainty level is consistent with applications for human motion modelling and simulations such as investigations into bone stresses and the related clinical implications (Jonkers et al. 2008). However, the sensitivity of forces calculated for each single muscle group was much higher with force variations reaching the same order of magnitude of the median calculated force. Therefore, conclusions taken on calculations of the muscle force magnitude should be considered cautiously.

The presented results compare well with published reports of intermediate findings. An earlier study (Taddei et al. 2007) reported an up to 2.3 mm inter- examiner variability in the location of the necessary bony landmarks, in good agreement with present findings. The joint kinematics showed an up to 11 degree variation, in good agreement with the 8 degree inter-examiner uncertainty reported by Della Croce et al. (1999). In their study, however, the authors used different optimization algorithms to calculate the instantaneous pose of each body segment from that used in this study. The much higher variation of muscle forces (up to 114%) than that of joint forces (9%) over their median value compares well with earlier studies (Brand et al. 1986; Herzog 1992). Brand et al. (1986) showed two to eight time variations in muscle forces and an up to 11% variation of the hip force by using different sets of the muscle physiological cross section area from different subjects. Herzog (1992) showed up to 100% variations of the calculated muscle forces resulting from perturbations of the muscle parameters within physiological boundaries.

This study has some limitations that may have affected the presented results. First, assuming the hip centre and the medio-lateral components of both the femoral epicondyles and the tibio-fibular malleoli as deterministic variables, might have led to smaller variations of all the calculated variables. This, however, allowed a drastic reduction of the number of simulations necessary to reach convergence. Moreover, the uncertainty on the estimation of the hip center is very small and the medio-lateral component of the femoral epicondyles and tibial malleoli has little effect on the knee and ankle axis orientations (Table 2), suggesting that these parameters are of secondary importance. Second, a specific image-based clinical procedure for identifying a specific musculoskeletal model comprising a fixed hinge at the knee and the ankle (Taddei et al., 2012) was studied. Different identification procedures and models (Delp et al., 1990) may be differently sensitive to the uncertainties on the joint parameters. Third, the results have been generated using one anatomical dataset. It is possible that the inclusion of additional subjects may lead to larger variations of all the investigated variables.

Despite the aforementioned limitations, the present findings provide the first quantitative comprehensive evaluation of the sensitivity of all the calculated lower-limb kinematics and kinetics variables to the inter-examiner uncertainty in defining the joint axes. By providing a better understanding of the reliability of the computed solution, these results could be helpful for those interested in human movement modelling and simulation, and contribute to a better informed decision- making process in clinical contexts.

In summary, the identification of the lower-limb joint axes through the location of prominent bony locations from CT images is a robust procedure to generate musculoskeletal models. Indeed, the sensitivity of the kinematics, the joint moments, and the joint forces to the joint axes uncertainty is moderate. However, conclusions based on calculated muscle forces should be interpreted with caution due to their higher sensitivity to joint axes uncertainties.

Conflict of interest

None of the authors has a conflict of interest in relation to this study.

Acknowledgment

We thank Irene Brambilla for the contribution to the preliminary analysis. This study was co-funded by the EC-funded projects NMSPhysiome (FP7 #24818965) and VPHOP (Grant #223865).

References

Brand RA, Pedersen DR, Friederich JA. 1986. The sensitivity of muscle forcepredictions to changes in physiologic cross-sectional area. J. Biomech. 19:589–596.

Della Croce U, Cappozzo A, Kerrigan DC. 1999. Pelvis and lower limb anatomicallandmark calibration precision and its propagation to bone geometry and joint angles.Med. Biol. Eng. Comput. 37:155–161.

Delp SL, Anderson FC, Arnold AS, Loan P, Habib A, John CT, Guendelman E, ThelenDG. 2007. OpenSim: open-source software to create and analyze dynamic simulationsof movement. IEEE Trans. Biomed. Eng. 54:1940–1950.

Delp SL, Loan JP, Hoy MG, Zajac FE, Topp EL, Rosen JM. 1990. An interactivegraphics-based model of the lower extremity to study orthopaedic surgical procedures.IEEE Trans. Biomed. Eng. 37:757–767.

Durkin JL, Dowling JJ. 2006. Body segment parameter estimation of the human lowerleg using an elliptical model with validation from DEXA. Ann. Biomed. Eng. 34:1483–1493.

Grood ES, Suntay WJ. 1983. A joint coordinate system for the clinical description ofthree-dimensional motions: application to the knee. J. Biomech. Eng. 105:136–44.

Herzog W. 1992. Sensitivity of muscle force estimations to changes in muscle inputparameters using nonlinear optimization approaches. J. Biomech. Eng. 114:267–268.

Jonkers I, Lenaerts G, Mulier M, Van der Perre G, Jaecques S. 2008. Relation betweensubject-specific hip joint loading, stress distribution in the proximal femur and bonemineral density changes after total hip replacement. J. Biomech. 41:3405–3413.

Leardini A, Cappozzo A, Catani F, Toksvig-Larsen S, Petitto A, Sforza V, Cassanelli G,Giannini S, 1999. Validation of a functional method for the estimation of hip jointcentre location. J. Biomech. 32:99–103.

Leardini A, Sawacha Z, Paolini G, Ingrosso S, Nativo R, Benedetti MG. 2007. A newanatomically based protocol for gait analysis in children. Gait Posture 26:560–71.

Lenaerts G, Bartels W, Gelaude F, Mulier M, Spaepen A, Van der Perre G, Jonkers I.2009. Subject-specific hip geometry and hip joint centre location affects calculatedcontact forces at the hip during gait. J. Biomech. 42:1246–1251.

Lenaerts G, De Groote F, Demeulenaere B, Mulier M, Van der Perre G, Spaepen A,Jonkers I. 2008. Subject-specific hip geometry affects predicted hip joint contact forcesduring gait. J. Biomech. 41:1243–1252.

Martelli S, Taddei F, Cappello A, van Sint Jan S, Leardini A, Viceconti M. 2011. Effectof sub-optimal neuromotor control on the hip joint load during level walking. J.Biomech. 44:1716–1721.

Scheys L, Loeckx D, Spaepen A, Suetens P, Jonkers I. 2009. Atlas-based non-rigidimage registration to automatically define line-of-action muscle models: a validationstudy. J. Biomech. 42:565–72.

Scheys L, Van Campenhout A, Spaepen A, Suetens P, Jonkers I. 2008. PersonalizedMR-based musculoskeletal models compared to rescaled generic models in the presenceof increased femoral anteversion: effect on hip moment arm lengths. Gait Posture28:358–365.

Taddei F, Ansaloni M, Testi D, Viceconti M. 2007. Virtual palpation of skeletallandmarks with multimodal display interfaces. Med. Inform. Internet Med. 32:191–8.

Taddei F, Martelli S, Valente G, Leardini A, Benedetti MG, Manfrini M, Viceconti M.2012. Femoral loads during gait in a patient with massive skeletal reconstruction. Clin.Biomech. (Bristol, Avon) 27:273–280.

Testi D, Quadrani P, Viceconti M. 2010. PhysiomeSpace: digital library service forbiomedical data. Philos. Trans. A. Math. Phys. Eng. Sci. 368:2853–61.

Testi D, Zannoni C, Cappello A, Viceconti M. 2001. Border-tracing algorithmimplementation for the femoral geometry reconstruction. Comput. Methods ProgramsBiomed. 65:175–82.

Valente G, Martelli S, Taddei F, Farinella G, Viceconti M. 2012. Muscle discretizationaffects the loading transferred to bones in lowerlimb musculoskeletal models. Proc. Inst.Mech. Eng. Part H J. Eng. Med. 226:161–9.

Viceconti M, Clapworthy G, Van Sint Jan S. 2008. The Virtual Physiological Human -a European initiative for in silico human modelling - A European Initiative for in silicoHuman Modelling. J. Physiol. Sci. 58:441–6.

Wu G, Siegler S, Allard P, Kirtley C, Leardini A, Rosenbaum D, Whittle M, D'LimaDD, Cristofolini L, Witte H, Schmid O, Stokes I. 2002. ISB recommendation ondefinitions of joint coordinate system of various joints for the reporting of human jointmotion--part I: ankle, hip, and spine. International Society of Biomechanics. J.Biomech. 35:543–548.

Table 1. The modelled muscles grouped according to their main function

Hip Abductors	Hip Adductors	Hip Extensors	Hip Flexors	Hip Rotators
Gluteus Medius	Adductor Brevis	Biceps Femoris Long Head	Iliacus	Gemellus
Gluteus Minimus	Adductor Longus	Gluteus Maximus	Psoas	Pectineus
Tensor Fascia Latae	Adductor Magnus	Semimembranosus	Rectus Femoris	Pyriform
	Gracilis	Semitendinosus	Sartorius	Quadratus Femoris
Knee Extensors	**Knee Flexors**	**Ankle Dorsiflexors**	**Ankle Plantarflexors**	
Rectus Femoris	Biceps Femoris Long Head	Extensor Digitorum	Flexor Digitorum	
Vastus Intermedius	Biceps Femoris Short Head	Extensor Hallucis	Flexor Hallucis	
Vastus Lateralis	Gastrocnemius	Peroneus Tertius	Gastrocnemius	
Vastus Medialis	Semimembranosus	Tibialis Anterior	Peroneus Brevis	
	Semitendinosus		Peroneus Longus	
			Soleus	
			Tibialis Posterior	

Table 2. Femoral epicondyles (LE, ME) and the tibial malleoli (LM, MM) position uncertainties and the consequent knee and ankle axis orientation uncertainties (STD (min:max)).

	Epicondyles position* (mm)	Knee axis orientation (deg)	Malleoli position* (mm)	Ankle axis orientation (deg)
medio-lateral (ML)	0.2 (-0.8:0.5)	0.2 (-0.5:0.4)	0.5 (-0.9:0.8)	0.4 (-0.8:0.7)
antero-posterior (AP)	2.0 (-4.8:6.4)	1.4 (-3.4:4.5)	2.3 (-4.6:3.5)	2.0 (-4.0:3.0)
cranio-caudal (CC)	1.4 (-4.2:3.4)	1.0 (-3.0:2.4)	1.4 (-1.7:3.0)	1.2 (-1.5:2.6)

* Epicondyle and malleoli positions are reported as standard-deviation (min:max) of the distances between the digitized positions and their respective averages. The standard deviation, the min and the max of the knee and ankle axes orientation are calculated using the epicondyles and malleoli standard-deviation, min and max along the ML, AP and CC coordinates and the average LE-ME and LM-MM distances for the knee and the ankle respectively.

Figure captions

Fig. 1. The comparison of calculated hip and muscle forces with publishedmeasurements and the available electromyography is taken from an earlier study(right) (Martelli et al. 2011). On the left, skeletal and skin geometriessuperimposed to the CT volume, a highlight of the identified lateral epicondyle(LE), and the OpenSim model during an intermediate frame of gait.

Fig. 2. Convergence curve for the joint reaction force at the knee (BW).Mean and SD are below the defined convergence thresholds 0.2% and 2%.

Fig. 3. The variation bands (top) and the range of variation (bottom) forthe joint angles. The stance and the swing phase are represents as well as the heelstrike (HS) and toe off (TO) instants. The discontinuity visible on the left jointangle patterns is due to the swap of the left stance and swing phase forcomparison purposes.

Fig. 4. The variation bands (top) and the range of variation (bottom) forthe joint moments. Calculated values are normalised as a percentage of the bodyweight (BW) times the subject high (H). The discontinuity visible on the left jointangle patterns is due to the swap of the left stance and swing phase forcomparison purposes. Stride phases are indicated as in Figure 3.

Fig. 5. The variation bands (top) and the range of variation (bottom) forthe muscle forces. The calculated values are normalised as a percentage of thebody weight (BW). Stride phases are indicated as in Figure 3.

Fig. 6. The variation bands (top) and the range of variation (bottom) forthe hip (A), the knee (B) and the ankle force (C). The calculated values arenormalised as a percentage of the body weight (BW). Stride phases are indicated as in Figure 3.

Figure 1

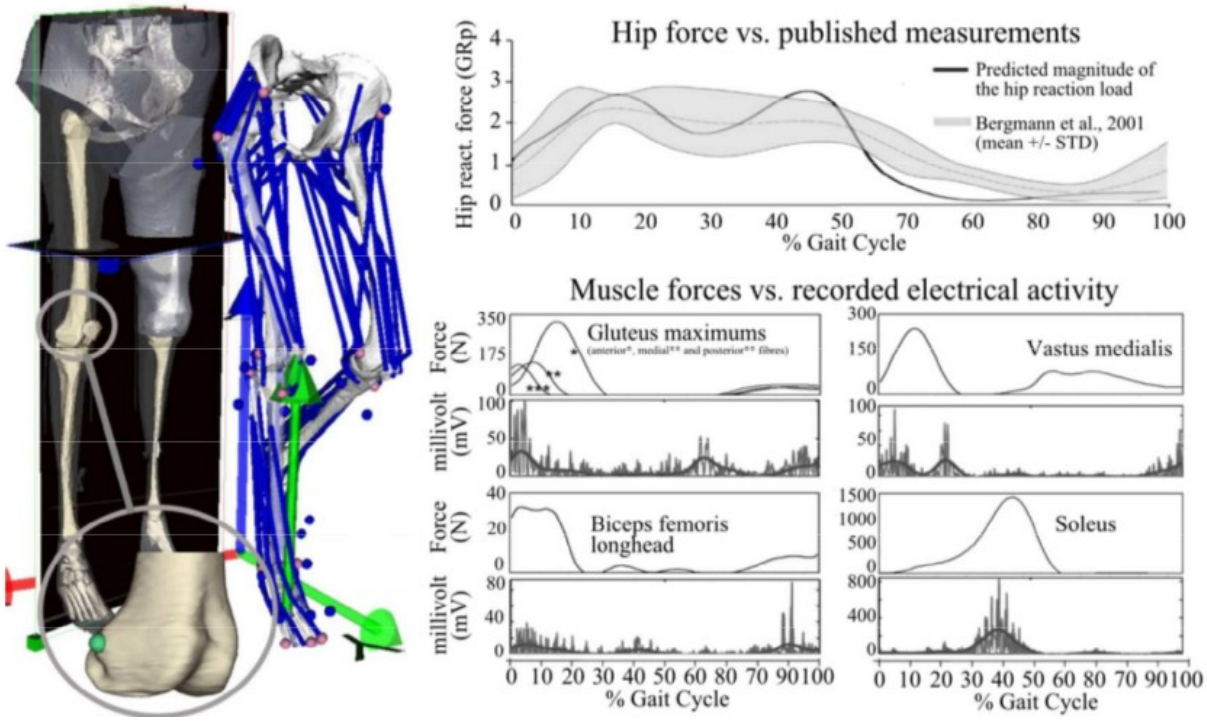
Hip force vs. published measurements
Hip react. force (GRp)
Predicted magnitude of the hip reaction load
Bergmann et al., 2001 (mean +/- STD)
% Gait Cycle
Muscle forces vs. recorded electrical activity
Force (N)
millivolt (mV)
Gluteus maximums
(anterior*, medial** and posterior** fibres)
Vastus medialis
Biceps femoris longhead
Soleus
% Gait Cycle
% Gait Cycle

Figure 2

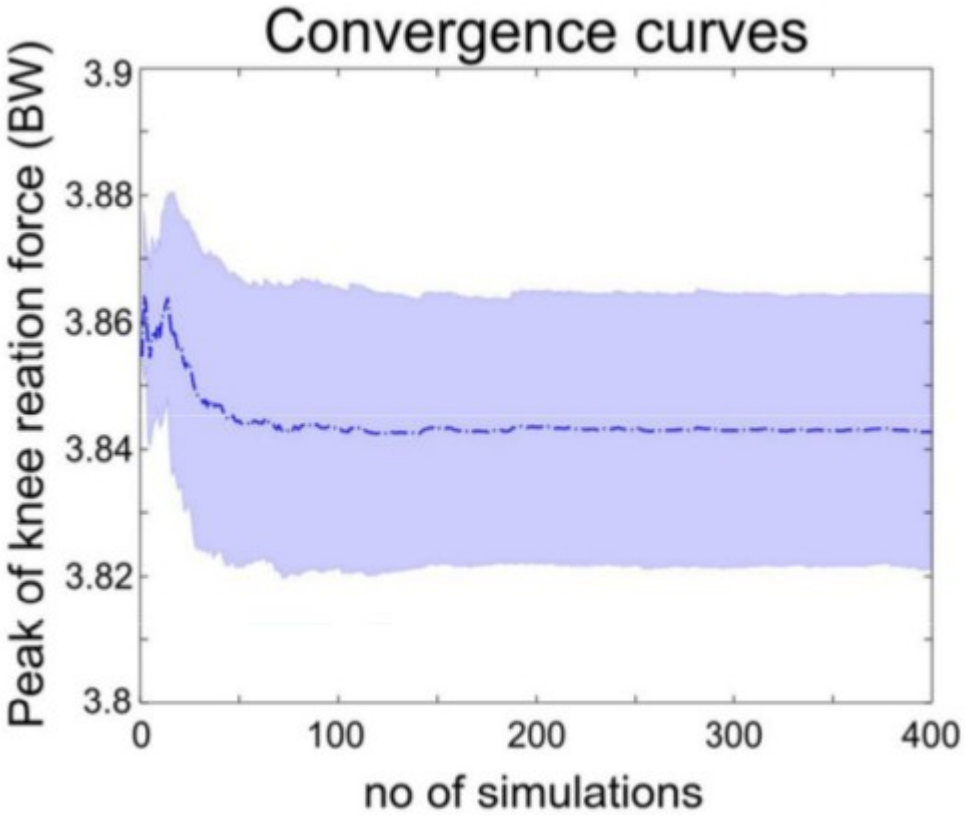
Convergence curves
Peak of knee reation force (BW)
3.9
3.88
3.86
3.84
3.82
3.8
0
100
200
300
400
no of simulations

Figure 3

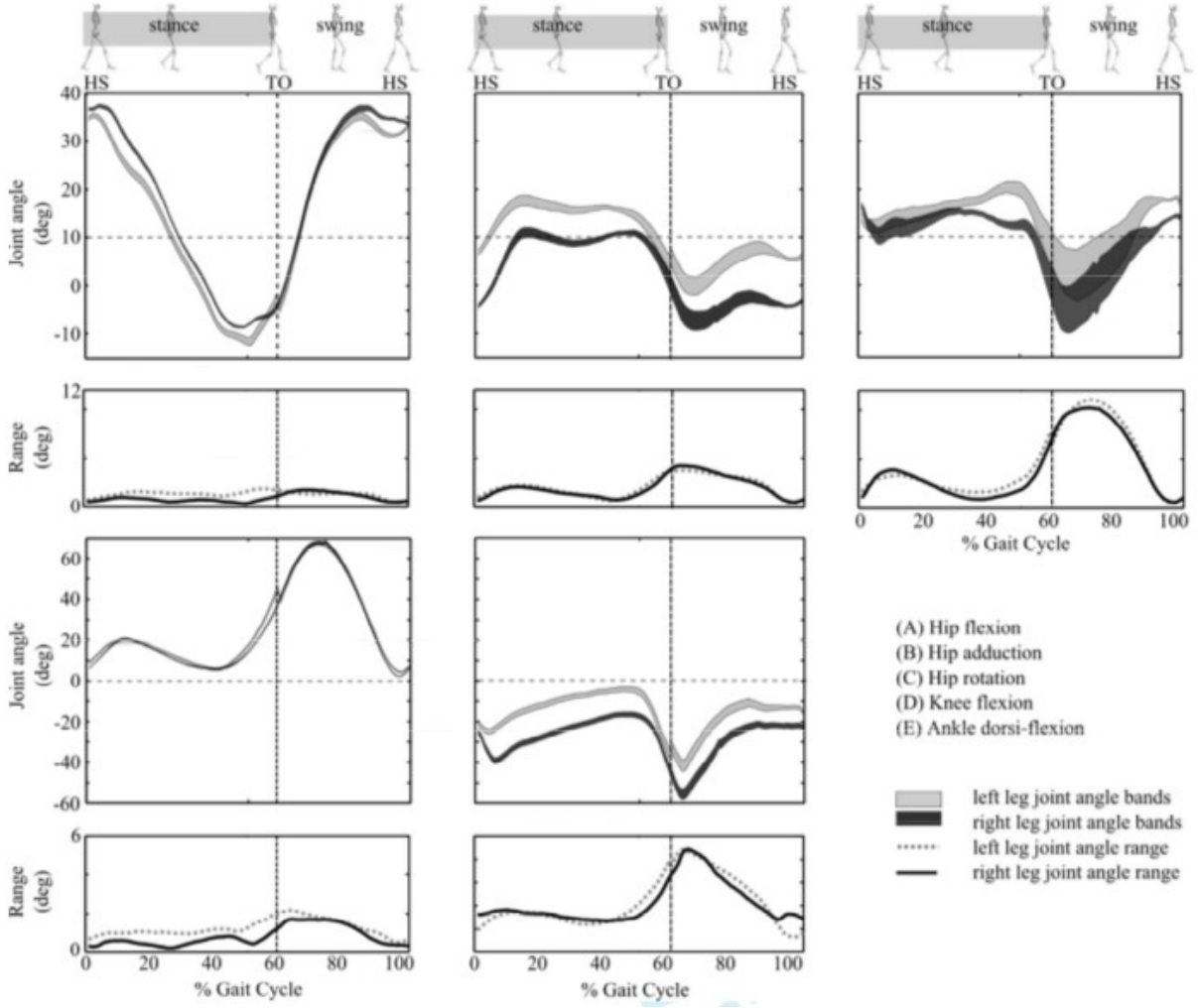
stance
swing
HS
TO
HS
Joint angle (deg)
Range (deg)
% Gait Cycle
(A) Hip flexion
(B) Hip adduction
(C) Hip rotation
(D) Knee flexion
(E) Ankle dorsi-flexion
left leg joint angle bands
right leg joint angle bands
left leg joint angle range
right leg joint angle range

Figure 4

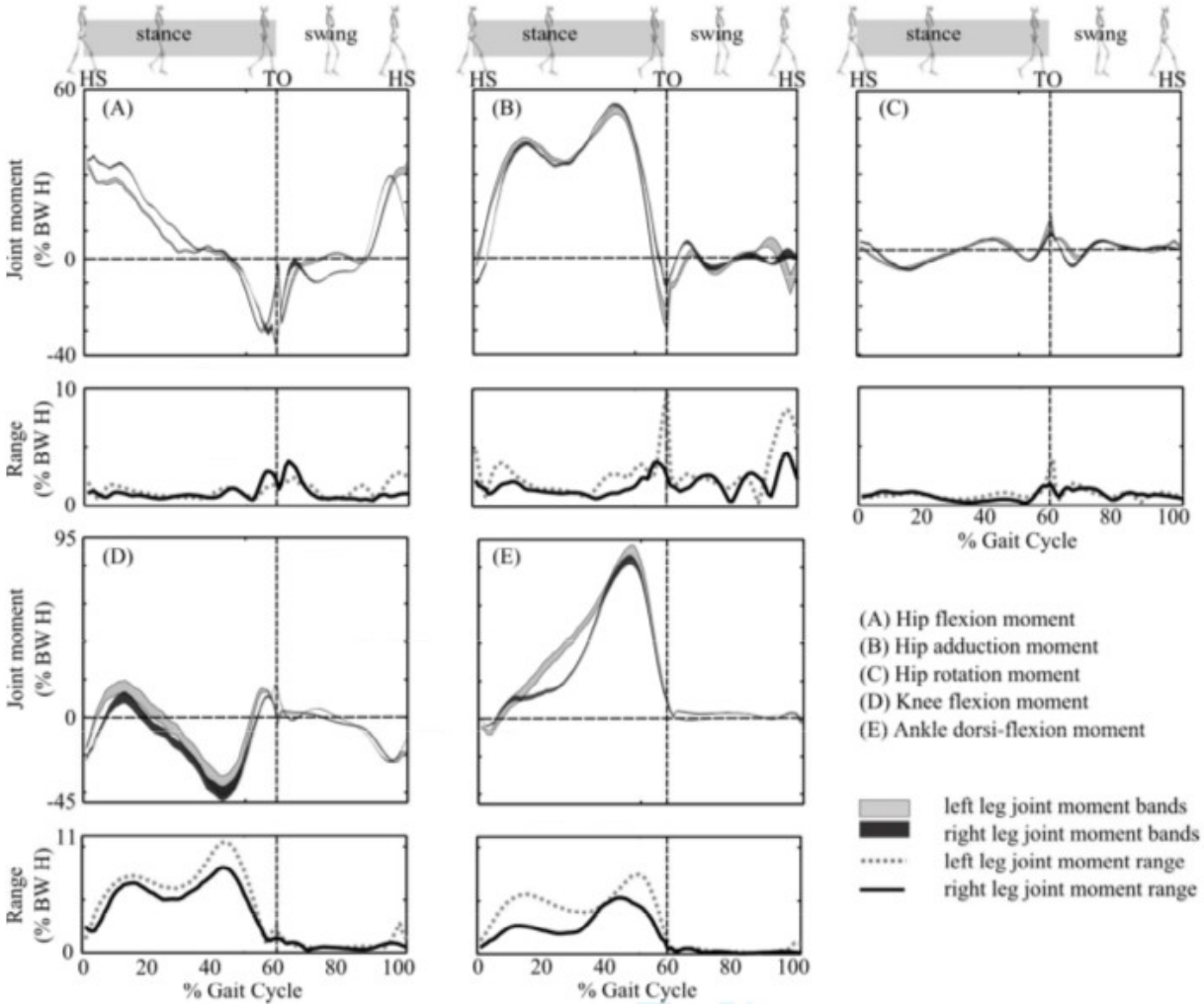
stance
swing
HS
TO
HS
(A)
(B)
(C)
(D)
(E)
Joint moment (% BW H)
Range (% BW H)
60
0
-40
10
0
95
0
-45
11
0
0 20 40 60 80 100
% Gait Cycle
(A) Hip flexion moment
(B) Hip adduction moment
(C) Hip rotation moment
(D) Knee flexion moment
(E) Ankle dorsi-flexion moment
left leg joint moment bands
right leg joint moment bands
left leg joint moment range
right leg joint moment range

Figure 5

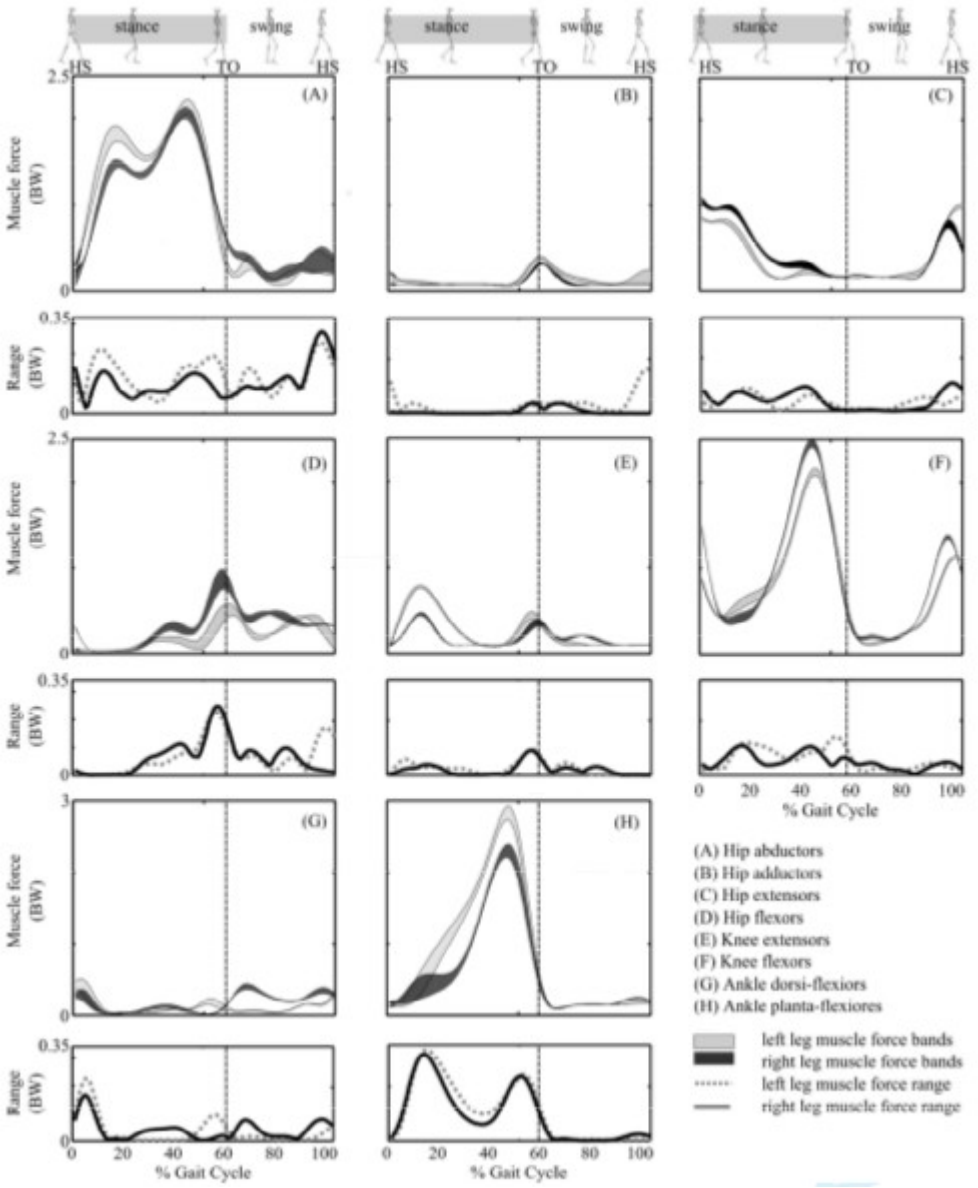
stance
swing
HS
TO
HS
(A)
(B)
(C)
(D)
(E)
(F)
(G)
(H)
Muscle force (BW)
Range (BW)
% Gait Cycle
(A) Hip abductors
(B) Hip adductors
(C) Hip extensors
(D) Hip flexors
(E) Knee extensors
(F) Knee flexors
(G) Ankle dorsi-flexiors
(H) Ankle planta-flexiores
left leg muscle force bands
right leg muscle force bands
left leg muscle force range
right leg muscle force range

Figure 6

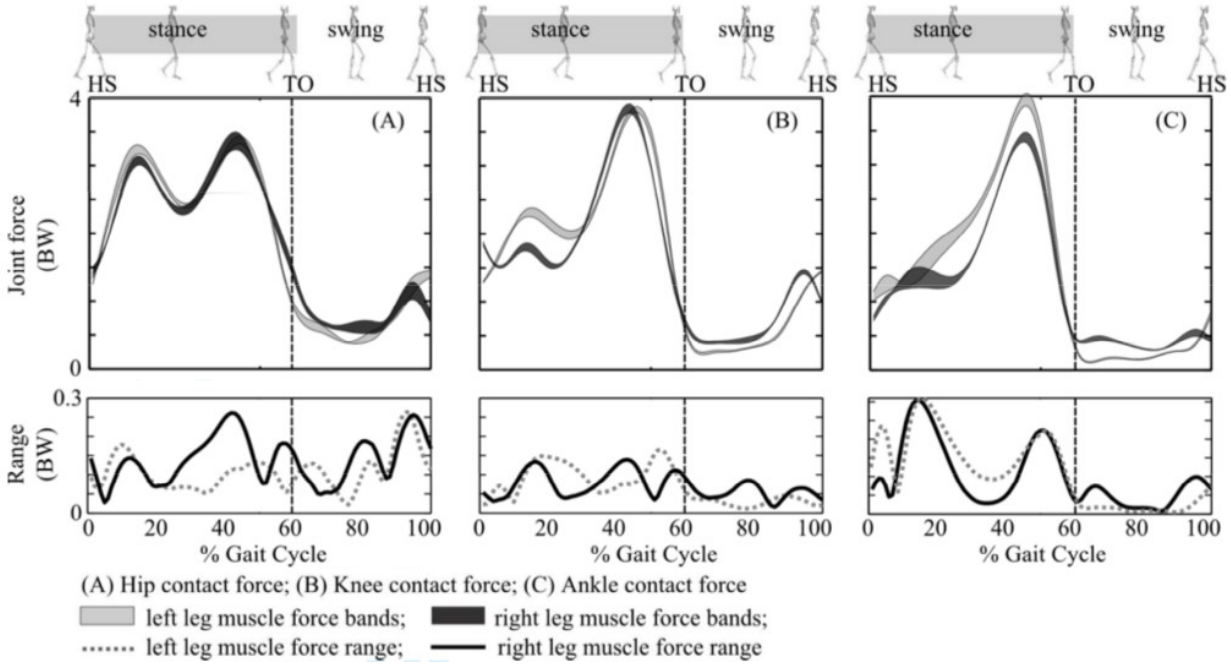
stance
swing
HS
TO
HS
(A)
(B)
(C)
Joint force (BW)
4
0
Range (BW)
0.3
0
0 20 40 60 80 100
% Gait Cycle
(A) Hip contact force; (B) Knee contact force; (C) Ankle contact force
left leg muscle force bands;
right leg muscle force bands;
left leg muscle force range;
right leg muscle force range